Supporting Information Materials and Methods

Mouse strains

The strains of *Zp3-Cre* and *Stra8-Cre* mice used in this study are FVB/N-TgN(Zp3-Cre)3Mrt and Tg(Stra8-cre)1Reb/J (Jackson labs) respectively. *Zp3*Cre and *Stra8*Cre are exclusively expressed in growing oocytes and spermatogonia respectively (1, 2), permitting the establishment of parental mouse strains with conditional *Tet1/3* deficiency only in female (*Zp3-Cre*) or male (*Stra8-Cre*) germ cells. *Zp3*-Cre and *Stra8*-Cre are expressed after PGC maturation (1, 2), later than the stage at which Tet1 is highly expressed and Tet3 is potentially involved (3, 4), thus bypassing any effects of *Tet1* and *Tet3* deletion on the methylation status and expression of imprinted genes. *Zp3-Cre* male mice and *Stra8-Cre* females did not generate deleted alleles, confirming the specificity of Cre expression. *Tet1$^{fl/fl}$,Tet3$^{fl/fl}$,Zp3-Cre* (*Zp3 DKO*) females and *Tet1$^{fl/fl}$,Tet3$^{fl/fl}$,Stra8-Cre* (*Stra8 DKO*) males were fertile; when mated with wild type mice, they gave rise to viable and fertile pups with double heterozygous alleles, confirming faithful germline deletion of the *Tet* floxed alleles. Moreover, *Tet3$^{fl/fl}$*,*Zp-3Cre* females bred to WT males produced normal *Tet3$^{+/-}$* pups in our mouse colony, with no indication of any maternal effects of oocyte-specific *Tet3* deletion as previously reported in *Tet3$^{fl/-}$*,*TNAP-Cre* and *Zp3-Cre* mice by embryo transfer (5). However, since *Zp3Cre* expression is turned on during oocyte development (1), we cannot exclude a maternal effect stemming from a potential decrease in Tet3 expression in oocytes; Tet1 and Tet2 are not detectable in oocytes (5), and so may not have a role.

The experimental breeders used in this study were *Zp3 DKO* females and *Stra8 DKO* males, which generate 100% *Tet1/3* DKO progeny, whereas the control breeders (*Tet1$^{fl/fl}$,Tet3$^{fl/fl}$*) were their Cre-negative littermates. We generated all females from matings of *Tet1$^{fl/fl}$,Tet3$^{fl/fl}$,Zp3-Cre* males to *Tet1$^{fl/fl}$,Tet3$^{fl/fl}$* females, and all males from the matings of *Tet1$^{fl/fl}$,Tet3$^{fl/fl}$,Stra8-Cre* females to *Tet1$^{fl/fl}$,Tet3$^{fl/fl}$* males, in each case yielding progeny of which 50% were Cre-negative and bore floxed alleles in their germ cells and 50% were Cre-positive and had deleted the floxed regions of both *Tet* alleles. Cre-negative animals were used as controls. This strategy was chosen because *Tet1$^{+/-}$*,*Tet3$^{+/-}$* matings yielded *Tet1/3* DKO embryos with very low frequency (1/16, an effect exacerbated by the small litter size).

Generation of *Tet1*- and *Tet3*- deficient mice

The endogenous *Tet1* locus was targeted for conditional excision of exons 8, 9, and 10 (***SI Appendix*, Fig. S1*A*, *top***). A targeting vector was designed to contain upstream/downstream homology arms, an FRT-flanked neomycin resistance cassette and *Loxp*-flanked central region (***SI Appendix*, Fig. S1*A*, *top***). *LoxP* sites were specifically inserted into introns upstream of exon 8 and downstream of exon 10 by standard gene targeting protocols. The linearized vector was electroporated into ART B6-3 ES cells with pure C57BL/6 NTac genetic background. In twenty-four hours, G418 selection enabled us to isolate resistant colonies of the ES clones, which then were expanded for screening. Using Southern blot analysis we identified the correct ES clones with homologous recombination mediated integration of targeting vector at the endogenous Tet1 locus as shown in ***SI Appendix*, Figure S1*A*, *top***. Blastocysts injected with the correct ES clones were implanted into B6-albino females and progeny with germline transmission were selected by coat color and PCR-genotyping from ear clips (***SI Appendix*, Fig. S1*A*, *bottom***). Mating between the targeted floxed allele mice and *FLP-E* deletor mice produced progeny deleted for the neomycin resistance cassette. The final step of breeding to *CMV-CRE* deletor mice produced Tet1 knockout mice with deletion of Tet1 exons 8–10 in all tissues. *Tet3*-deficient mice were generated similarly (***SI Appendix*, Fig. S1*B*)**.

Embryo collection, immunofluorescence and microscopy

Mice were sacrificed and dissected as directed in the laboratory animal protocol. All subsequent steps were performed at room temperature. After timed matings, dissected oviducts (E2.5) or uteri (E3.5 and E4.5) were flushed with 6 μg/ml BSA containing PBS. Embryos were removed from zona pellucida using acidic Tyrode's solution (Sigma, T1788) under a dissecting microscope (Leica), plated on coverslips coated with 0.2% gelatin, then **(a)** fixed/permeabilized with 1% paraformaldehyde (PFA) and 0.05% NP-40 in PBS for

10 min or **(b)** fixed with 4% PFA in PBS for 10 min and subsequently permeabilized with 0.2% NP-40 in PBS for 5 min, blocked for 1 hr using a PBS-based blocking buffer containing 5% donkey serum, 0.2% fish skin gelatin and 0.2% Tween-20, then sequentially incubated with primary and secondary antibodies in the same blocking buffer for 2 hr and 0.5 hr respectively. Between antibody incubation steps, the coverslips were washed 3 times with PBS-T (0.2% Tween-20) for 5 min. The coverslips were treated for 5 min with DAPI (5 µg/ul) diluted 1:5000 in PBS-T, washed with PBS-T, and mounted using mounting medium (Vectashield). For 5mC and 5hmC staining, nuclear DNA was denatured with 2N HCl for 30 min and then neutralized with 100 mM Tris-HCl, pH 8 for 10 min. Subsequent staining steps were the same as same as described above, except that the blocking buffer was 1%BSA/0.05% Tween-20 in PBS and the washing buffer was 0.05% Tween-20 in PBS. Images were recorded using either Olympus FV10i confocal or Marianas microscope, and processed using imageJ software.

Late-stage embryos were dissected and frozen using the O.C.T. (optimal cutting temperature) compound in the cryomold. Multiple sections of embryos were plated on the slide in the cryostat. The following antibodies are used at the indicated diluting ratio: α-NANOG (1:100, BD Pharmingen 560259), α-CDX2 (1:100, BioGenex MU392A-UC), α-GATA6 (1:50, R&D Systems AF1700), α-Tet1 (1:100, GeneTex GTX125888; 1:500 Millipore 09-872), α-Tet3 (1:100, GeneTex GTX121453), α-5hmC (1:500, Active motif 39791), α-5mC (1:100, Epigenetek A-1014), α-Srebp2 (1:300, GeneTex GTX82865, 1:100 Abcam ab30682), pS139-γH2AX (1:100, Biolegend 613408). Alexafluor 488, 555 and 647 secondary antibodies (1:300, Invitrogen).

Single- embryo and cell RNA sequencing

CTL and *Tet1/3* DKO 8-cell embryos and blastocysts were collected at E2.5 and E3.5 respectively. 8-cell embryos were dissociated using a 1:1 mixture of 10X TrypLE and Collagenase (Life technology). Single cells or embryos were lysed and converted into double stranded cDNA using SMARTer ultra low RNA kit for Illumina sequencing (Clontech). 1 ng of cDNA for each sample was used for preparing libraries using Nextera XT DNA sample preparation kit (Illumina). The good quality of the prepared libraries was validated using the Bioanalyzer high sensitivity DNA kit (Agilent). Then, the library was sequenced using an Illumina HISEQ 2500 instrument. RNA-seq data were mapped against mm9 using Tophat (v. 2.0.0*, -g 1, --mate-std-dev=70, --no-coverage-search, --library-type=fr-unstranded*) by providing a RefSeq gene annotation obtained from the UCSC data base (11/07/2014). Sequencing read counts per gene were calculated using htseq-count *(-m union -s no -t exon -i gene_id*).

Analysis of gene expression variability

To identify genes with high variance across samples independent of their expression strength, we performed variance-stabilizing transformation using the *varianceStabilizingTransformation* function available in DESeq (6). Based on this variance-stabilized data (vsd), principal component analysis (PCA) was computed in R using the svd (singular value decomposition) function applied to the top 400 or 500 variable genes. In order to avoid the influence of the gender of the embryos on the PCA, we excluded the genes (**see Fig. 6*C***) of the sex chromosomes prior to the analysis.

For the comparison of single-cell gene expression data with expression profiles from zygotes, 2-cell, and 4-cell stage embryos (7), single-cell RNA-seq data was downloaded from NCBI Gene Expression Omnibus (GEO, http://www.ncbi.nlm.nih.gov/geo/, accession number GSE57249) and was further processed as described above. We repeated the principal component analysis based on variance-stabilized data (vsd) of the top 500 variable genes across the zygote, 2-cell, 4-cell stage embryos (7), and our 8-cell control samples. Subsequently, we projected the gene expression data of the *Tet1/3* DKO cell samples onto the principal components.

Differential expression

Differential gene expression has been assessed using the *nbinomTest* function of the R bioconductor library DESeq (6). Subsequently, p-values have been adjusted for multiple testing by applying the R function 'p.adjust', using the method of Benjamini and Hochberg (method='BH')(8). In order to analyze differential expression of transposable elements, Mus musculus and ancestral (shared) repeat sequences were downloaded from Repbase (http://www.girinst.org/repbase/update/browse.php, Repeat Class: All; Included Elements: autonomous, non-autonomous, simple; Taxon: Mus Musculus; Output Format: FATSA) RNA-seq reads were aligned to these references using Bowtie 0.12.9 (9) (-y -m 10 -k10 --best --chunkmbs 1000), and the reads per sequence were counted. Differential expression of transposable elements was calculated analogous to differential gene expression using DESeq.

Single-embryo reduced-representation bisulfite sequencing (RRBS)

Single embryos and 100 fg lambda spike-in DNA (Fermentas) were lysed in the lysis buffer (20 mM Tris-EDTA (pH 8.0), 20 mM KCl, and 0.3% Triton X-100, 1 mg/mL protease (Qiagen)) for 3 h at 50°C and then heat-inactivated for 30 min at 75°C. Released gDNA was treated using 10 U MspI (NEB) in 15 µL reaction for 3 h at 37°C and prepared for RRBS libraries using the Ovation® Ultralow Methyl-Seq Library (Nugen). The good quality of the prepared libraries was validated using the Bioanalyzer high sensitivity DNA kit (Agilent). Then, the library was sequenced using an Illumina HISEQ 2500 instrument.
RRBS reads have been trimmed using trim_galore version 0.3.3 with parameters for RRBS (--rrbs).
The reads were aligned to a combined reference from mouse NCBI37/mm9 and lambda J02459.1 genomes using Bismark v0.10.0 (10), based on bowtie 2.2.1. The *Bismark_methylation_extractor* script of the Bismark software was used to analyze methylation at CpGs. For each sample, the number of reads covering methlyated and unmethylated CpGs where counted in each chromosome, in promoter regions (TSS +/- 2kb), in CpG islands as defined by G. Miklem and L. Hillier in http://rafalab.jhsph.edu/CGI/ in TFBS downloaded from chipBase (http://deepbase.sysu.edu.cn/chipbase/chipSeq.php, mouse/mm9 at 2014/04/25), and in lambda genome, respectively.

Bisulfite sequencing and CMS dot blot assay

Single embryos were lysed using the lysis buffer in the EZ DNA Methylation-Direct™ Kit (Zymo research). Then, bisulfite treatment was conducted as directed in the provider's manual. The following primers were used: Nanog TSS (5'GGGATTAATTGTGAATTTATAGGG and 5' AAAAAAACCCACACTCATATCA), Nanog enhancer (5'TGGATAAGGAATGTAGTAAGTTTG and 5'CCAAAAAACTAACTAATTCAAACTC), Srebp2 TSS (5' GAGGTTTTTAGTTTTTTTGGTT and 5' ATCTCTATCCACTCCATCAATA) and Srebp2 enhancer (5'TTTTGATATTTTATTGTTTGGAGG and 5'CCTCCCCCTAACTCTAAATAAA). Amplicons were subcloned into PCR4-topo plasmids and sequenced.

For the CMS dot blot assay (11, 12), cells were incubated with lysis buffer (10 mM Tris (pH8.0), 100 mM NaCl, 2.5 mM EDTA, 0.5% SDS, 200 µg/mL proteinase K and 10 µg/mL RNAse) at 55°C overnight followed by phenol-chloroform extraction. Purified genomic DNA was bisulfite-treated using the Methylcode bisulfite conversion kit (Invitrogen). The bisulfite-converted DNA was further denatured in 0.4 M NaOH, 10 mM EDTA at 95°C for 10 min and neutralized in 2M ammonium acetate (pH 7.0). These DNA samples were serially diluted by two-fold and then spotted on a nitrocellulose membrane using Bio-Dot apparatus (Bio-Rad). DNA spots on the membrane were fixed by vacuum baking at 80°C for 2 hr. To detect CMS on the spots, the membrane was blocked with 5% nonfat milk and subsequently incubated with homemade anti-CMS antiserum (1:2,000). After 3 TBS-T washes for 5 min, the membranes were incubated with HRP-conjugated anti-rabbit IgG secondary antibody. All incubation steps were done for 1 hr at room temperature. CMS was detected on X-ray films after treatment of the membranes with HRP substrates, ECL (Perkin Elmer).

Methylation-sensitive restriction digest

CTL and Tet1/3 DKO E10.5 embryos were lysed in buffer containing 10 mM Tris (pH8.0), 100 mM NaCl, 2.5mM EDTA, 0.5% SDS, 200 μg/mL proteinase K and 10 μg/mL RNase. Genomic DNA was prepared, digested with *BstU1* and PCR amplification was conducted as described (13). Briefly, 1 μg DNA was digested in NEBuffer4 using 0.5 U *BstUI* (NEB) at 60℃ for 2 h, which was inactivated with 1 μL Proteinase K (10 mg/mL) at 50℃ for 2 h. The reaction was stopped by incubation at 95℃ for 10 min.

Quantitative real time PCR

Total RNA was extracted using TRIzol reagent (Invitrogen) according to the manufacturer's instructions. 0.5~1 μg RNA was used for cDNA synthesis catalyzed by SuperScript III (Invitrogen). 1/40 of cDNA was added to Universal SYBR Green Master mix (Roche) and analyzed by StepONE plus real-time PCR system (Applied Biosystems). All the intron-spanning qPCR primers in this study were designed and generated via *Integrated DNA technologies, Inc* (http://www.idtdna.com/site).

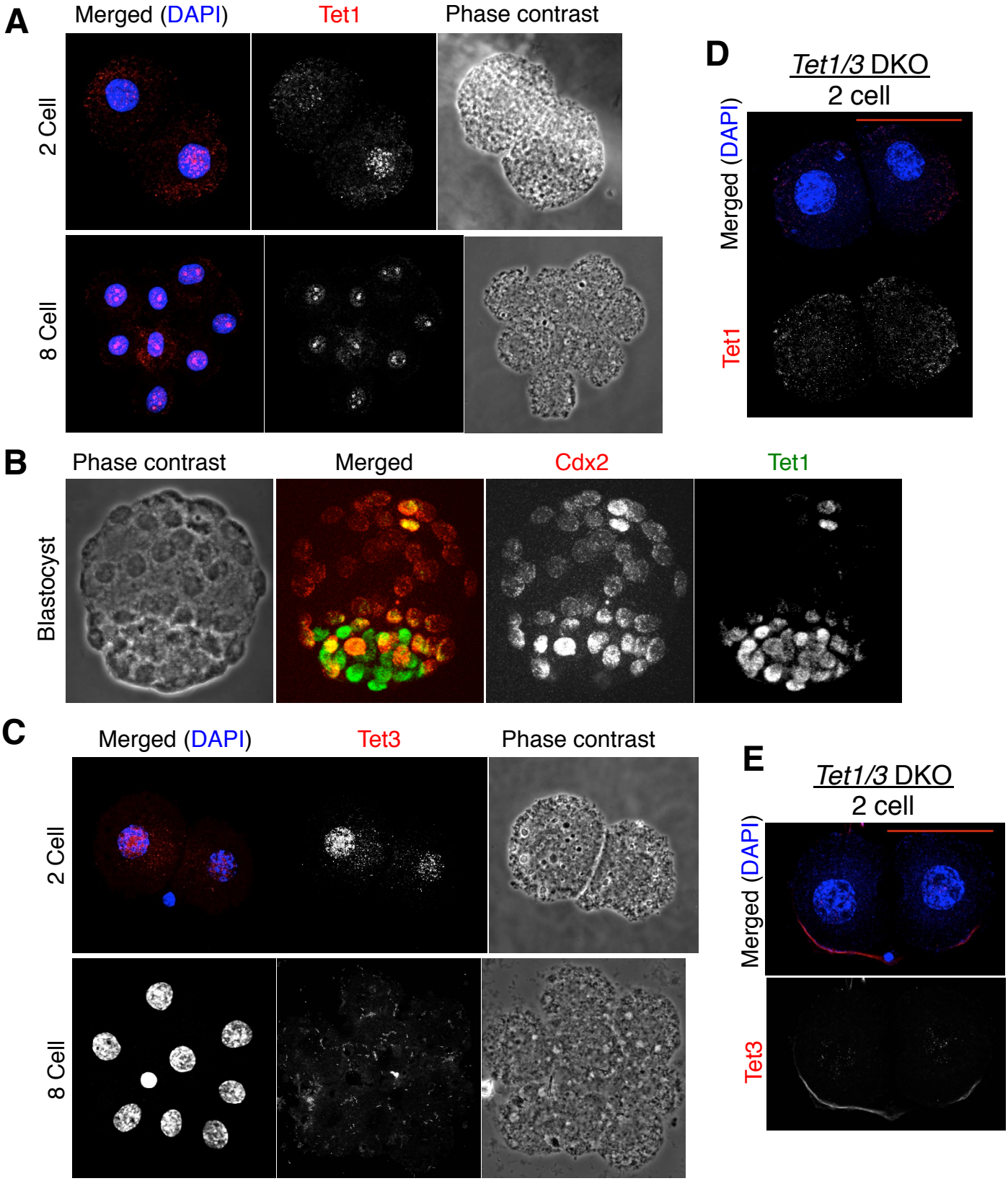

Figure S1. Tet1 and Tet3 expression in preimplantation embryos evaluated by immunocytochemistry using specific antibodies. (**A**) Tet1 is expressed in both 2-cell and 8-cell embryos. (**B**) Tet1 is expressed in the blastocyst. (**C**) Tet3 is expressed in the 2-cell but not the 8-cell embryo. Note potential asymmetric distribution of Tet1 and Tet3 at the 2-cell stage. (**D**, **E**) The specificity of the Tet1 (**D**) and Tet3 (**E**) antibodies was confirmed by showing lack of staining of a *Tet1/3* DKO 2-cell embryo. Scale bar 50 μm.

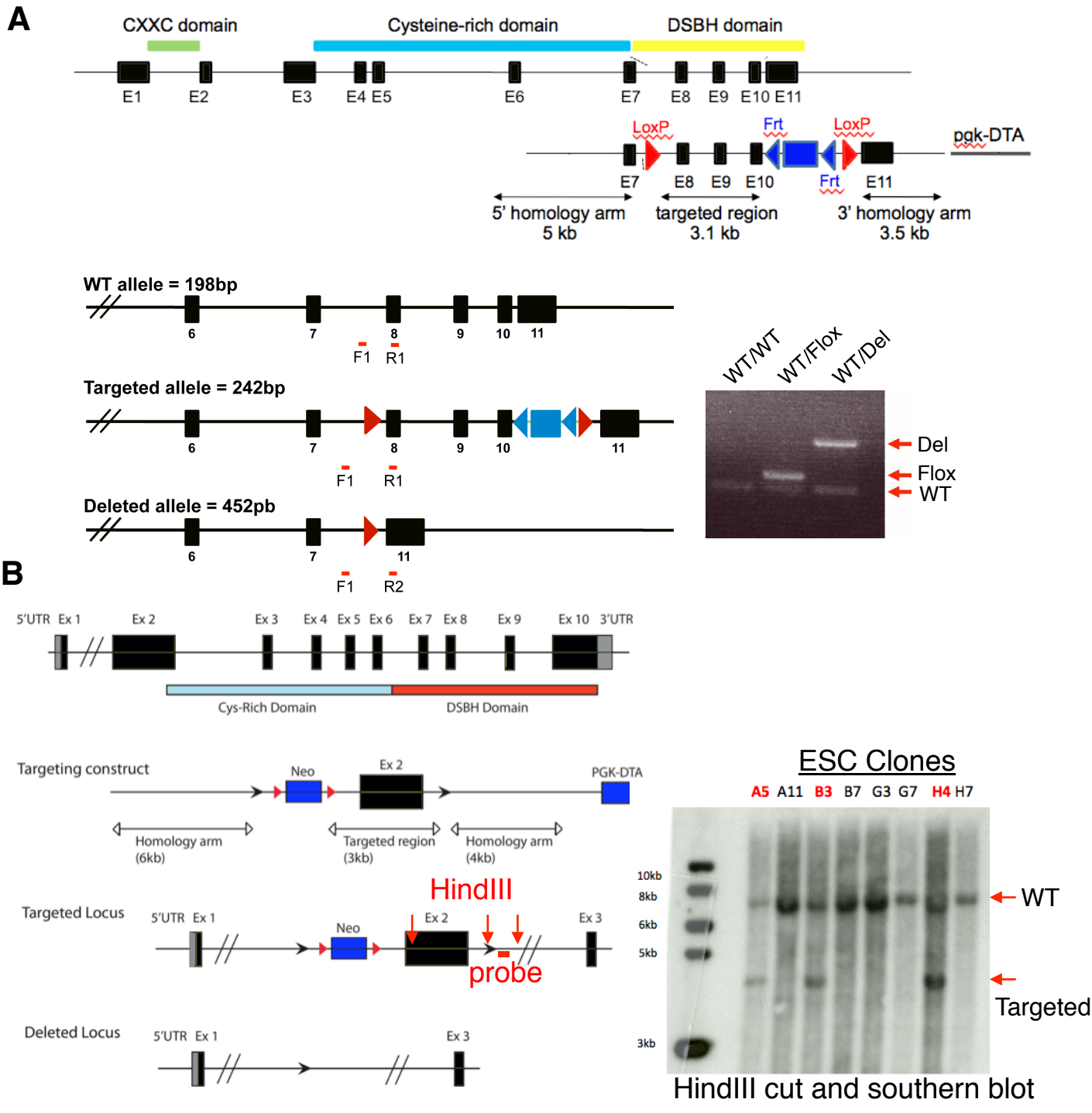

Figure S2. Generation of *Tet1* KO and *Tet3* KO mice. (**A**) *Top*, Schematic view of targeting vector and targeting scheme for deletion of exons 8-10 in the endogenous *Tet1* locus*; Bottom*, Positions of PCR primers at *Tet1* locus (F1, R1) discriminating WT, floxed and deleted alleles. PCR result is shown at right. Detailed protocols are described in *Methods*. (**B**) *Left*, Schematic view of targeting vector and targeting scheme for deletion of exon 2 in the endogenous *Tet3* locus; *Right*, Screening for targeted ES clones by Southern blot.

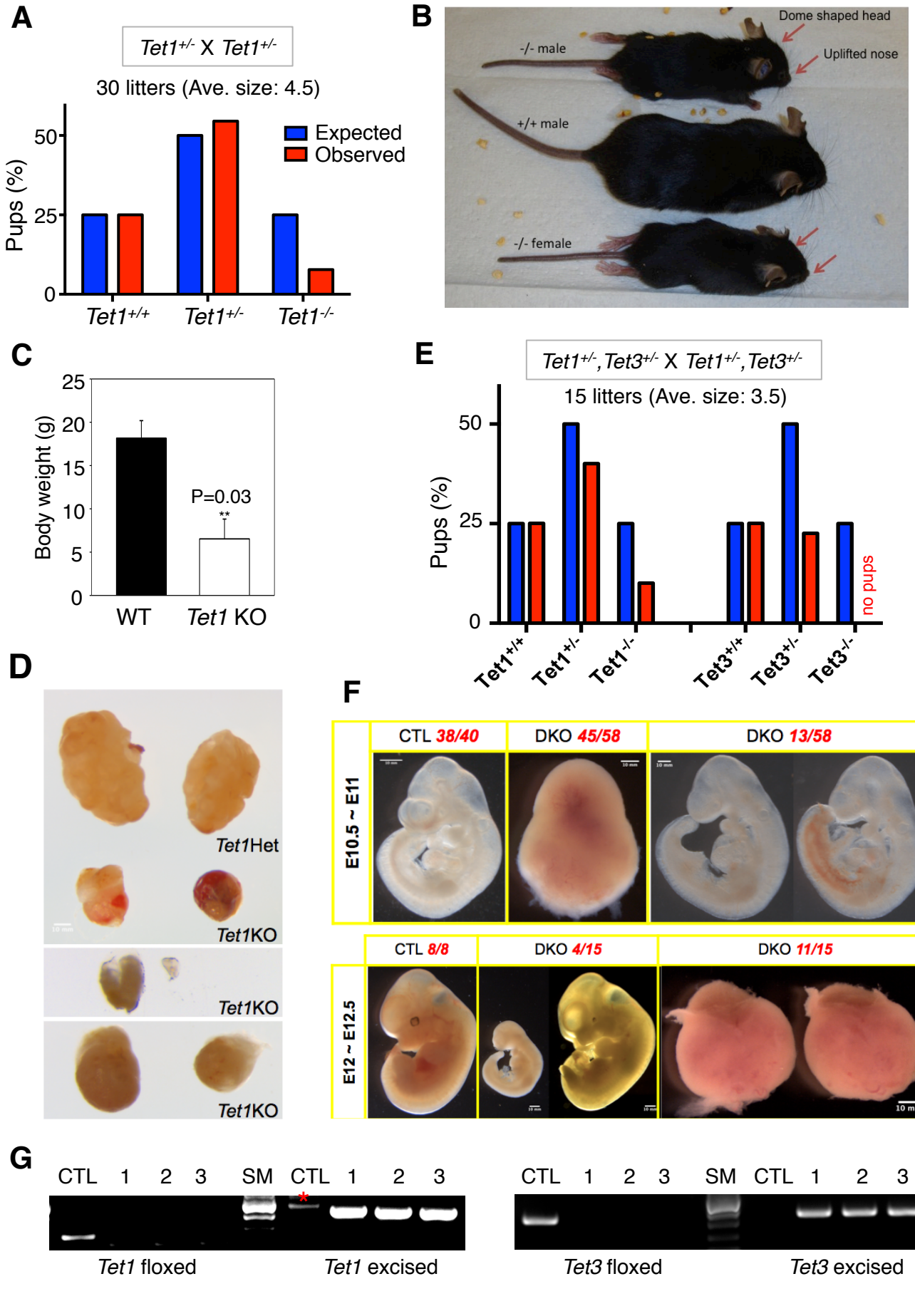
A
Tet1+/- X Tet1+/-
30 litters (Ave. size: 4.5)
Pups (%)
50
25
0
Expected
Observed
Tet1+/+
Tet1+/-
Tet1-/-
B
Dome shaped head
Uplifted nose
-/- male
+/+ male
-/- female
C
Body weight (g)
25
20
15
10
5
0
P=0.03
**
WT
Tet1 KO
D
Tet1Het
Tet1KO
Tet1KO
Tet1KO
E
Tet1+/-,Tet3+/- X Tet1+/-,Tet3+/-
15 litters (Ave. size: 3.5)
Pups (%)
50
25
0
no pups
Tet1+/+
Tet1+/-
Tet1-/-
Tet3+/+
Tet3+/-
Tet3-/-
F
E10.5 ~ E11
CTL 38/40
DKO 45/58
DKO 13/58
E12 ~ E12.5
CTL 8/8
DKO 4/15
DKO 11/15
10 mm
G
CTL 1 2 3 SM CTL 1 2 3
Tet1 floxed
Tet1 excised
CTL 1 2 3 SM CTL 1 2 3
Tet3 floxed
Tet3 excised

Figure S3. Phenotypes of *Tet1* KO and *Tet3* KO mice. (**A**) Bar graph summarizing frequency of *Tet1* genotypes from the *Tet1*$^{+/-}$ breedings (see ***SI Appendix*, Table S1**). (**B**) Whole body appearance of WT male and *Tet1* KO male and female mice (red arrows indicate typical symptoms of hydrocephaly). (**C**) Comparison of body weights of WT and *Tet1* KO mice (n=3). (**D**) *Tet1* Het and *Tet1* KO ovaries are dissected and compared (age of around 2.5 month). (**E**) Bar graph summarizing frequency of *Tet1* and *Tet3* genotypes from the *Tet1*$^{+/-}$,*Tet3*$^{+/-}$ breedings (see ***SI Appendix*, Table S2**). Because the *Tet1* allele on chromosome 10 and the *Tet3* allele on chromosome 6 are independently inherited, their inheritance frequencies can be calculated separately. As previously noted (5), *Tet3*$^{+/-}$ matings yielded *Tet3*$^{+/-}$ and *Tet3*$^{-/-}$ pups at the expected Mendelian frequencies, but *Tet1*$^{+/-}$, *Tet3*$^{+/-}$ double-heterozygous matings yielded no *Tet3*$^{-/-}$ pups and *Tet3*$^{+/-}$ pups were born at half the expected frequency, indicating that concurrent Tet1 deficiency exacerbates the impaired phenotypes of mice carrying *Tet3* mutant alleles. (**F**) *Top row*, At E10.5~E11, 38/40 control (CTL) embryos had a normal appearance (*left*), but 45/58 *Tet1/3* DKO embryos were resorbed in decidua (*middle*), whereas the remaining 13/58 embryos appeared to be developing (*right*). *Bottom row*, At E12-E12.5, all CTL embryos were normal (*left*); *Tet1/3* DKO embryos appeared to be decaying and did not display any heartbeat (*middle*); were resorbed (*right*). (**G**) PCR genotyping for *Tet1* (*left*) and *Tet3* (*right*) alleles in E10.5 CTL and 3 *Tet1/3* DKO embryos. * indicates nonspecific amplification with different size.

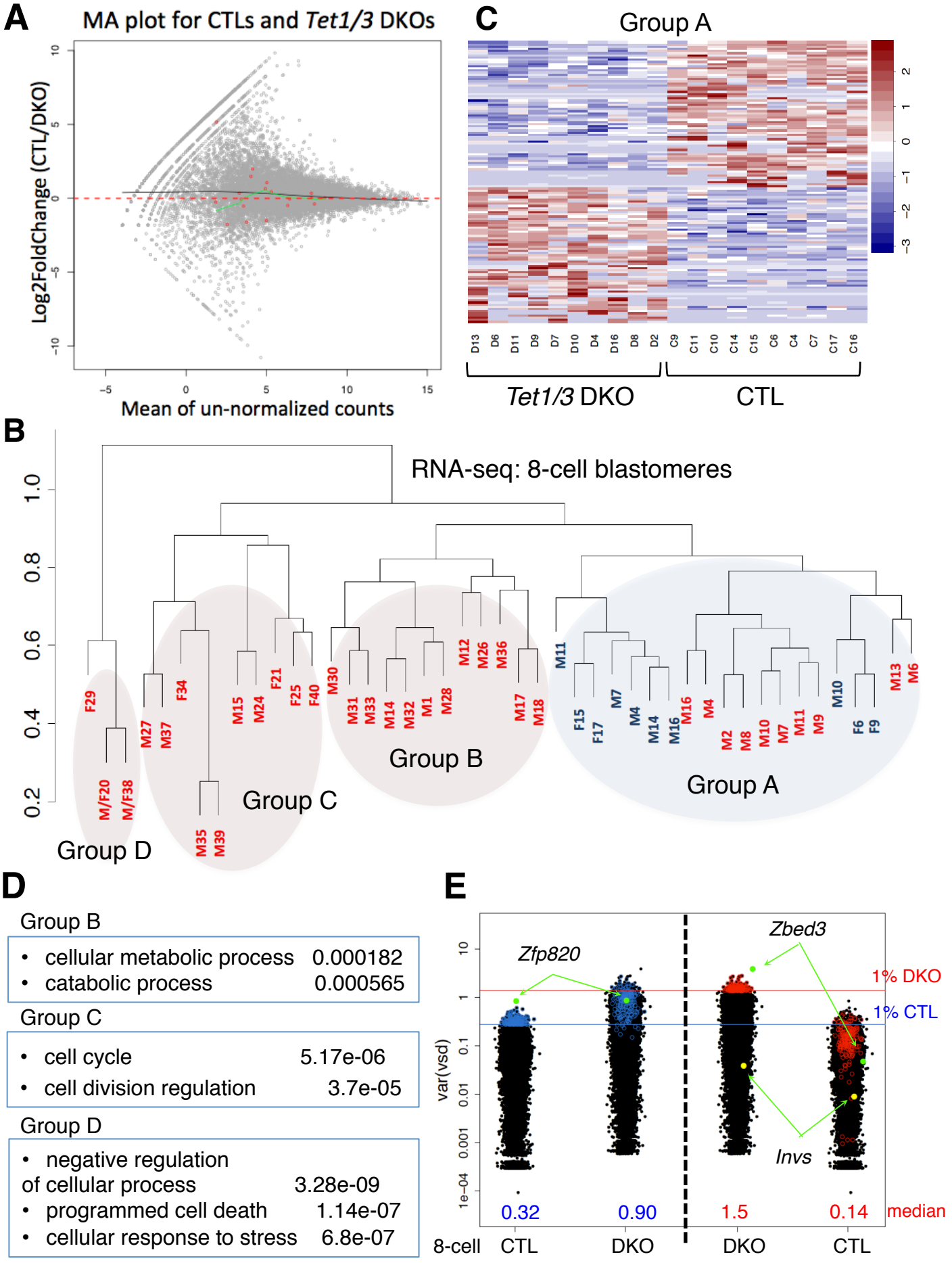
A
MA plot for CTLs and Tet1/3 DKOs
Log2FoldChange (CTL/DKO)
Mean of un-normalized counts
C
Group A
D13 D6 D11 D9 D7 D10 D4 D16 D8 D2
C9 C11 C10 C14 C15 C6 C4 C7 C17 C16
Tet1/3 DKO
CTL
B
RNA-seq: 8-cell blastomeres
F29 M/F20 M/F38 M27 M37 F34 M35 M39 M15 M24 F21 F25 F40 M30 M31 M33 M14 M32 M1 M28 M12 M26 M36 M17 M18 M11 F15 F17 M7 M4 M14 M16 M16 M4 M2 M8 M10 M7 M11 M9 M10 F6 F9 M13 M6
Group D
Group C
Group B
Group A
D
Group B
• cellular metabolic process 0.000182
• catabolic process 0.000565
Group C
• cell cycle 5.17e-06
• cell division regulation 3.7e-05
Group D
• negative regulation of cellular process 3.28e-09
• programmed cell death 1.14e-07
• cellular response to stress 6.8e-07
E
Zfp820
Zbed3
Invs
1% DKO
1% CTL
var(vsd)
0.32 0.90 1.5 0.14 median
8-cell CTL DKO DKO CTL

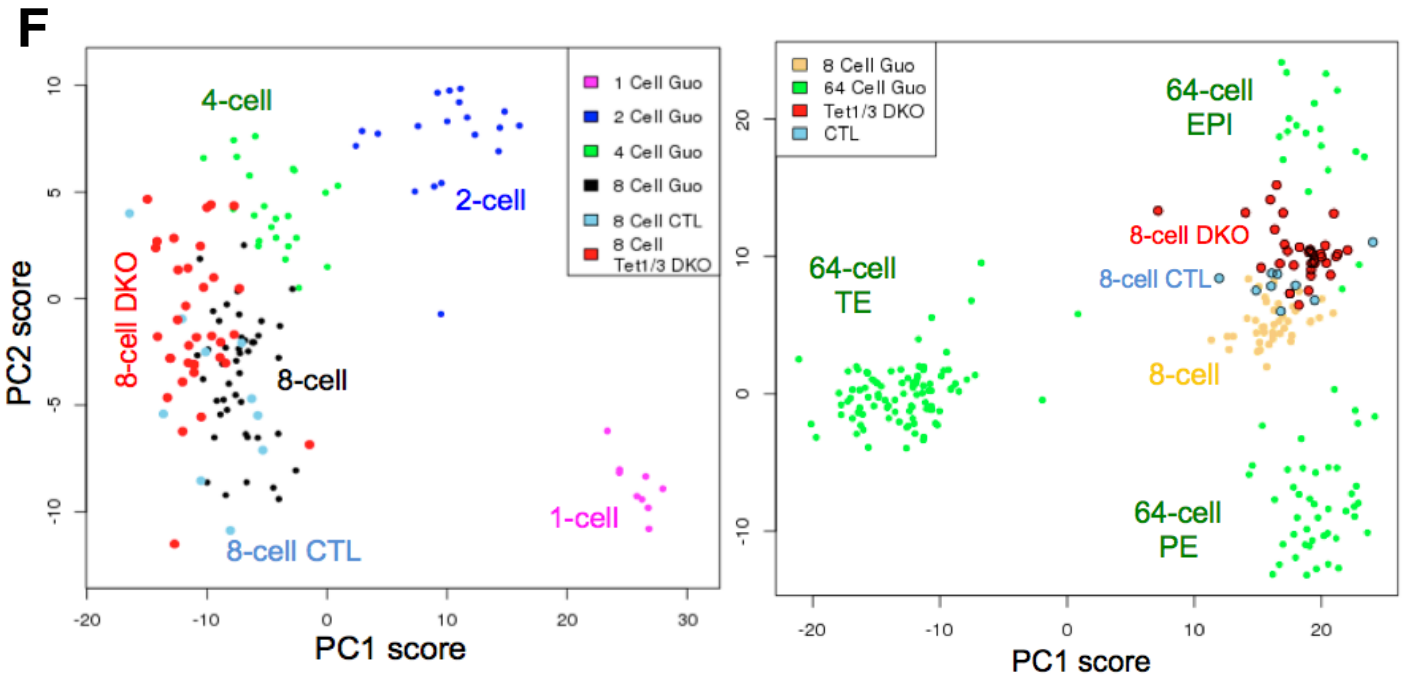

Figure S4. Analyses of RNA-seq data from single cells (blastomeres) of 8-cell embryos. (**A**) Log-scaled MA plot showing the FoldChange of un-normalized read counts (CTL, DKO) against average un-normalized read counts. The grey symbols represent the genes and red symbols represent the ERCC spike-ins. Only ERCC spike-ins with an average un-normalized read count greater than 2 were considered. The lines are the lowest local regression fits for genes (black) and spike-ins (green). The red spike-in controls are scattered around the zero line, indicating that there is no global increase of expression in the DKO group. (**B**) Unsupervised clustering analysis based on single-cell RNA-seq, using the top 400 differentially-expressed genes. Each blastomere is indicated by its number and sex (M/F, based on expression of sex chromosome genes shown in ***SI Appendix*, Figure S6*C***). The dendrogram separates 4 distinct groups. (**C**) Heatmap of differentially expressed genes between the 10 CTL and 10 *Tet1/3* DKO blastomeres in Group A. (**D**) GO analysis was applied to the genes differentially expressed in groups B, C and D compared to group A, which includes all control blastomeres. The GO categories are displayed with p-values. (**E**) The top 1% of variable genes in CTL cells (*blue dots*, *left*) and *Tet1/3 DKO* cells (*red dots*, *right*) are shown on the variance-stabilization dot plot. The median variances of these selected genes (blue and red dots) are shown at the bottom. The top variable genes (*Zfp820* and *Zbed3* in CTL and DKO blastomeres respectively) and a stably-expressed gene (*Invs*) are indicated; the expression levels of these genes are shown in **Figure 2*E***. (**F**) *Left panel*, Expression levels of the 48 genes analyzed by Guo *et al*. (2010) were extracted from the RNA-seq data for the individual DKO and CTL blastomeres analyzed in this study, and projected onto a PCA plot of gene expression (RNA-seq) from the 1-cell (zygote) to the 8-cell embryo obtained by Guo *et al.* (2010). *Right panel*, A similar combined PCA plot that includes the 64-cell blastomere distribution pattern from Guo *et al*. (2010).

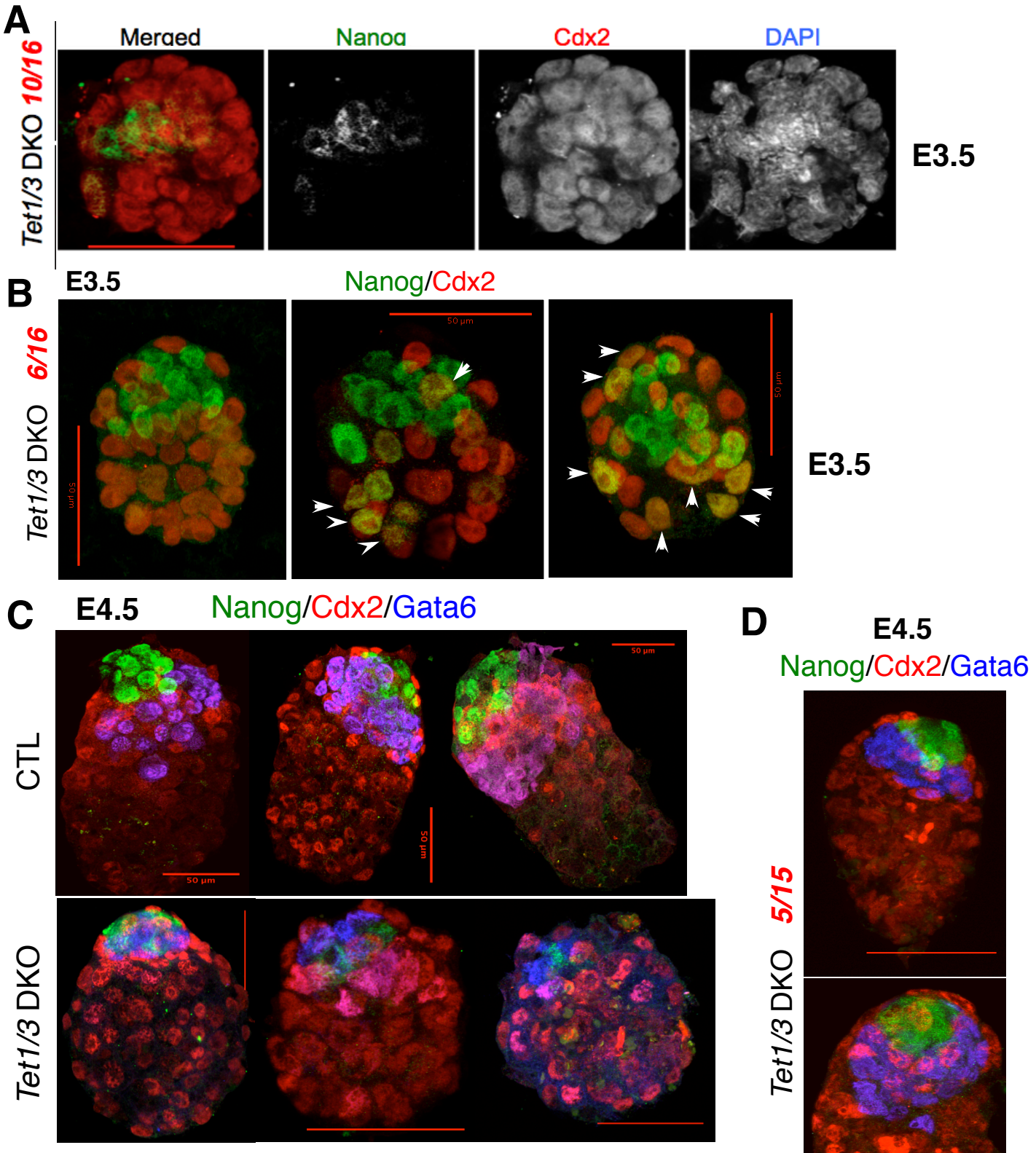

Figure S5. Additional examples of Nanog, Cdx2 and Gata6 staining at E3.5 and E4.5. (**A**) Another example of a failed *Tet1/3* DKO blastocyst stained for Nanog and Cdx2. (**B**) A few E3.5 *Tet1/3* DKO embryos show high levels of Nanog expression (6 out of 16 *Tet1/3* DKO embryos). Arrows indicate abnormal co-expression of Nanog and Cdx2. (**C**) Merged images of CTL (*top row*) and *Tet1/3* DKO (*bottom row*) E4.5 embryos stained for Nanog, Cdx2 and Gata6. (**D**) E4.5 *Tet1/3* DKOs with relatively normal appearance but abnormally small size, stained for Nanog, Cdx2 and Gata6 (5 out of 15 *Tet1/3* DKO embryos). Scale bar 50 μm.

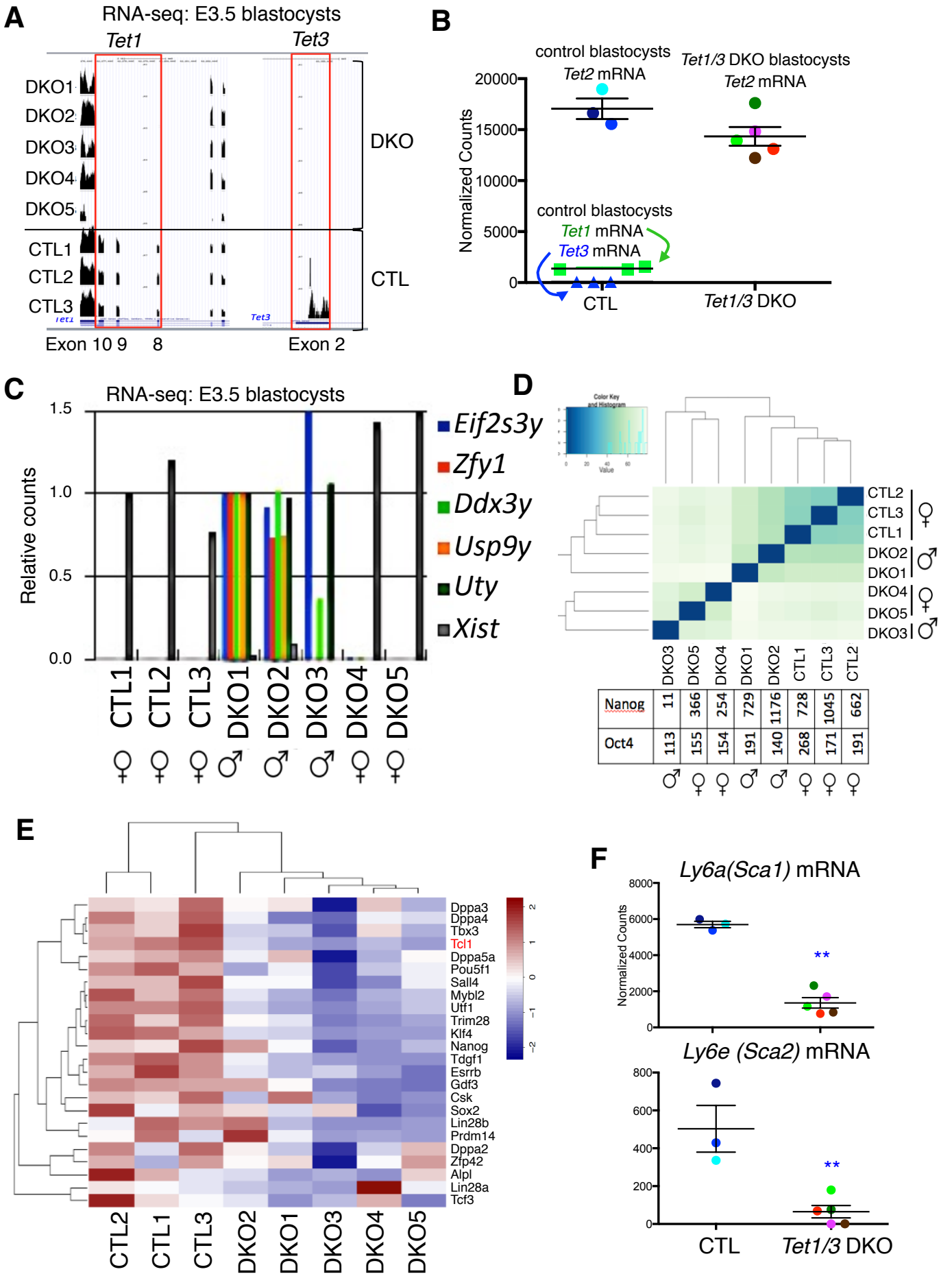
A
RNA-seq: E3.5 blastocysts
Tet1
Tet3
DKO1
DKO2
DKO3
DKO4
DKO5
DKO
CTL1
CTL2
CTL3
CTL
Exon 10 9 8
Exon 2
B
control blastocysts
Tet2 mRNA
Tet1/3 DKO blastocysts
Tet2 mRNA
Normalized Counts
20000
15000
10000
5000
0
control blastocysts
Tet1 mRNA
Tet3 mRNA
CTL
Tet1/3 DKO
C
RNA-seq: E3.5 blastocysts
Relative counts
1.5
1.0
0.5
0.0
Eif2s3y
Zfy1
Ddx3y
Usp9y
Uty
Xist
CTL1
CTL2
CTL3
DKO1
DKO2
DKO3
DKO4
DKO5
D
Color Key and Histogram
Value
CTL2
CTL3
CTL1
DKO2
DKO1
DKO4
DKO5
DKO3
DKO3 DKO5 DKO4 DKO1 DKO2 CTL1 CTL3 CTL2
Nanog 11 366 254 729 1176 728 1045 662
Oct4 113 155 154 191 140 268 171 191
E
Dppa3
Dppa4
Tbx3
Tcl1
Dppa5a
Pou5f1
Sall4
Mybl2
Utf1
Trim28
Klf4
Nanog
Tdgf1
Esrrb
Gdf3
Csk
Sox2
Lin28b
Prdm14
Dppa2
Zfp42
Alpl
Lin28a
Tcf3
2
1
0
−1
−2
CTL2
CTL1
CTL3
DKO2
DKO1
DKO3
DKO4
DKO5
F
Ly6a(Sca1) mRNA
Normalized Counts
8000
6000
4000
2000
0
**
Ly6e (Sca2) mRNA
800
600
400
200
0
**
CTL
Tet1/3 DKO

Figure S6. Analyses of single-embryo RNA-seq. (**A**) Genome browser snapshots showing RNA-seq reads for targeted exons of *Tet1* and *Tet3*. Reads corresponding to *Tet1* exons 9,10 and 11 and *Tet3* exon 2 are specifically missing in *Tet1/3* DKO blastocysts. The expression level of Tet3 is very low, thus reads are only observed in 2/3 CTL embryos. (**B**) *Tet1, Tet2* and *Tet3* mRNA expression levels in CTL embryos and *Tet2* mRNA levels in *Tet1/3* DKO embryos assessed by RNA-seq. Note the high expression of *Tet2* mRNA relative to the low expression of *Tet1* mRNA and the almost absent expression of *Tet3* mRNA in CTL blastocysts. (**C**) Expression levels of Y chromosome genes and *Xist* from the RNA-seq data for each embryo. The sex of each embryo is determined by the pattern of expression of Y chromosome genes and *Xist*. (**D**) Unsupervised clustering of transcriptome data for 3 CTL and 5 *Tet1/3* DKO blastocysts. *Bottom*, the table shows the expression levels of *Nanog* and *Oct4* matched to the individual embryos on the cluster chart. (**E**) Heatmap showing expression of 24 different pluripotency-related genes in CTL and *Tet1/3* DKO blastocysts. The *Tcl1* gene is indicated in red. (**F**) *Ly6a* (*Sca1*, *top*) and Ly6e (*Sca2*, *bottom*) expression is significantly impaired in *Tet1/3* DKO embryos compared to controls (taken from RNA-seq data; adjusted p-value < 0.01).

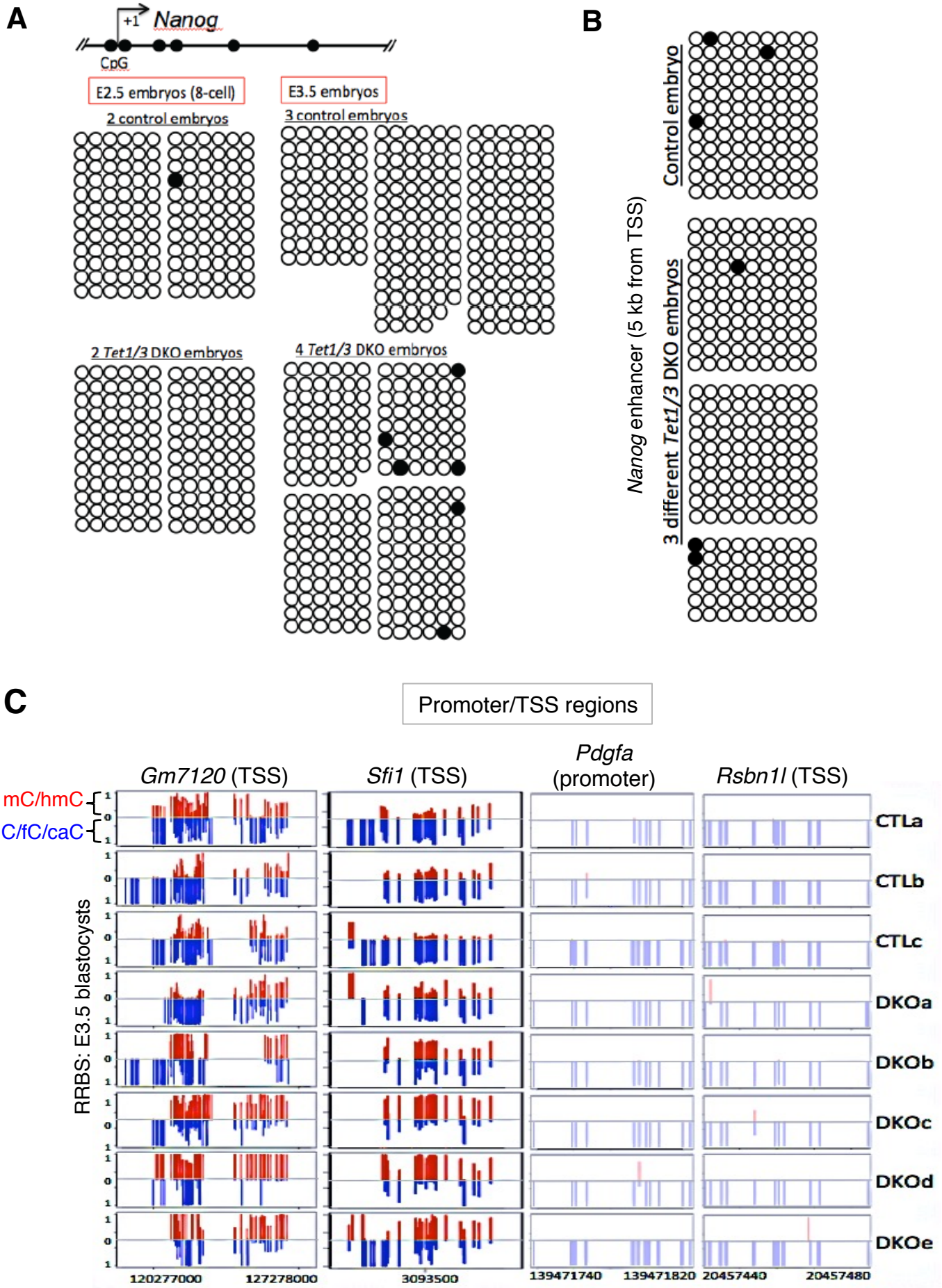
A
+1
Nanog
CpG
E2.5 embryos (8-cell)
2 control embryos
E3.5 embryos
3 control embryos
2 Tet1/3 DKO embryos
4 Tet1/3 DKO embryos
B
Control embryo
3 different Tet1/3 DKO embryos
Nanog enhancer (5 kb from TSS)
C
Promoter/TSS regions
Gm7120 (TSS)
Sfi1 (TSS)
Pdgfa (promoter)
Rsbn1l (TSS)
mC/hmC
C/fC/caC
RRBS: E3.5 blastocysts
CTLa
CTLb
CTLc
DKOa
DKOb
DKOc
DKOd
DKOe
120277000
127278000
3093500
139471740
139471820
20457440
20457480

Figure S7. Analyses of DNA modifications in single-embryos. (**A**) Near-complete demethylation of the *Nanog* TSS region in several individual CTL and *Tet1/3* DKO embryos at both E2.5 and E3.5 stages. (**B**) Near-complete demethylation of the *Nanog* distal regulatory region, analyzed in 1 CTL and 3 *Tet1/3* DKO E3.5 embryos. (**C**) The promoter/TSS regions of *Gm7120, Sfi1, Pdgfa* and *Rsbn1l* show either variable DNA modification or nearly complete demethylation (C/5fC/5caC) in both control and *Tet1/3* DKO blastocysts as judged by RRBS. CpGs covered by at least 8 reads were analyzed and the fraction of unconverted (5mC+5hmC; *red bars*) and converted (C+5fC+5caC; *blue bars*) cytosines in CpGs is shown, with the summed length of the blue and red bars set at 1.

Figure S8

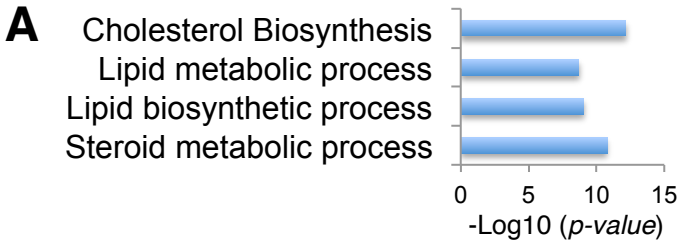
A
Cholesterol Biosynthesis
Lipid metabolic process
Lipid biosynthetic process
Steroid metabolic process
0
5
10
15
-Log10 (p-value)

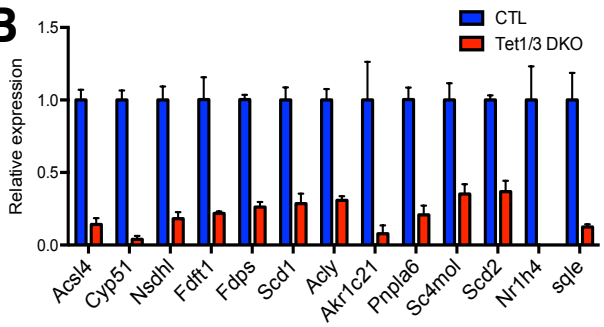
B
CTL
Tet1/3 DKO
Relative expression
1.5
1.0
0.5
0.0
Acsl4
Cyp51
Nsdhl
Fdft1
Fdps
Scd1
Acly
Akr1c21
Pnpla6
Sc4mol
Scd2
Nr1h4
sqle

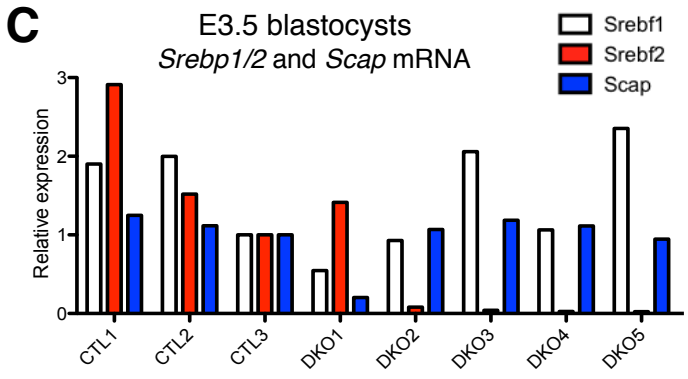
C
E3.5 blastocysts
Srebp1/2 and Scap mRNA
Srebf1
Srebf2
Scap
Relative expression
3
2
1
0
CTL1
CTL2
CTL3
DKO1
DKO2
DKO3
DKO4
DKO5

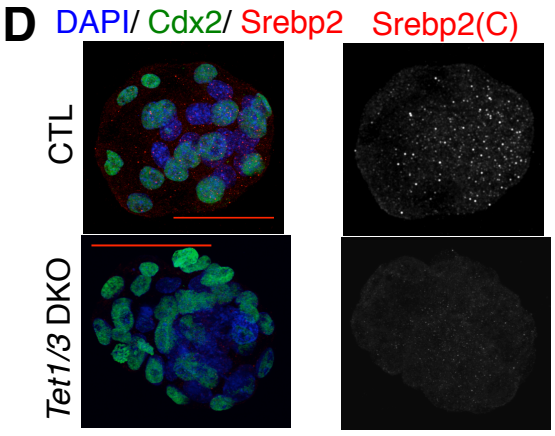
D
DAPI/ Cdx2/ Srebp2
Srebp2(C)
CTL
Tet1/3 DKO

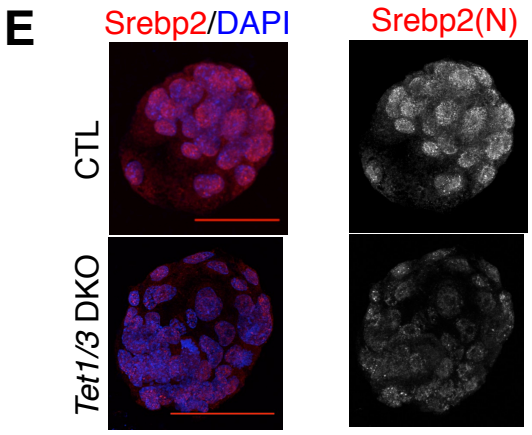
E
Srebp2/DAPI
Srebp2(N)
CTL
Tet1/3 DKO

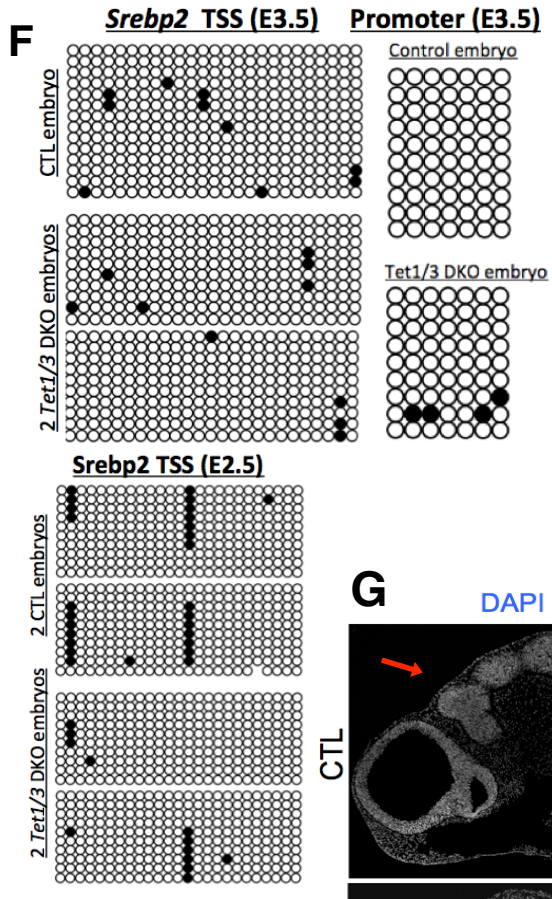
F
Srebp2 TSS (E3.5)
Promoter (E3.5)
Control embryo
CTL embryo
Tet1/3 DKO embryo
2 Tet1/3 DKO embryos
Srebp2 TSS (E2.5)
2 CTL embryos
2 Tet1/3 DKO embryos

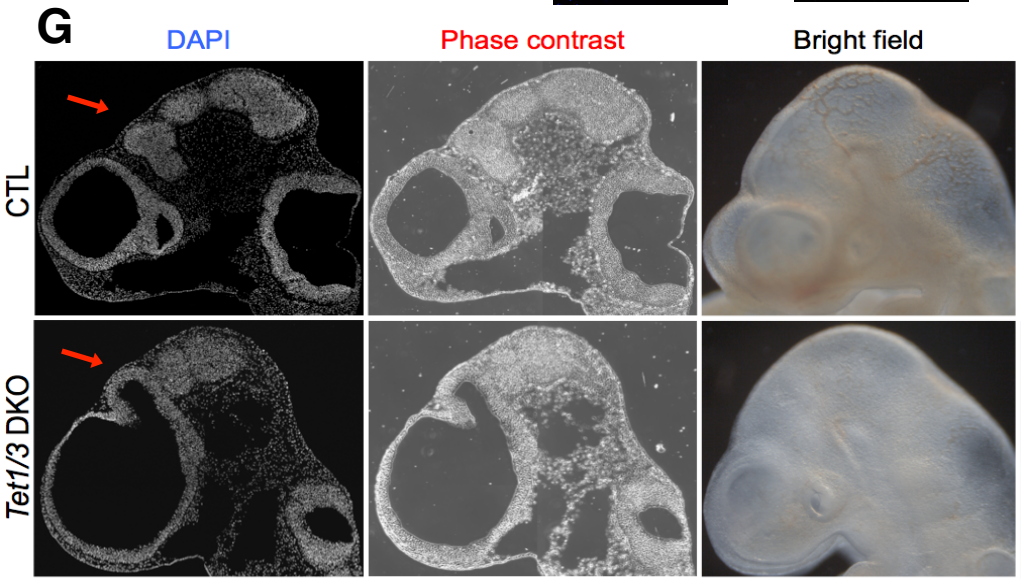
G
DAPI
Phase contrast
Bright field
CTL
Tet1/3 DKO

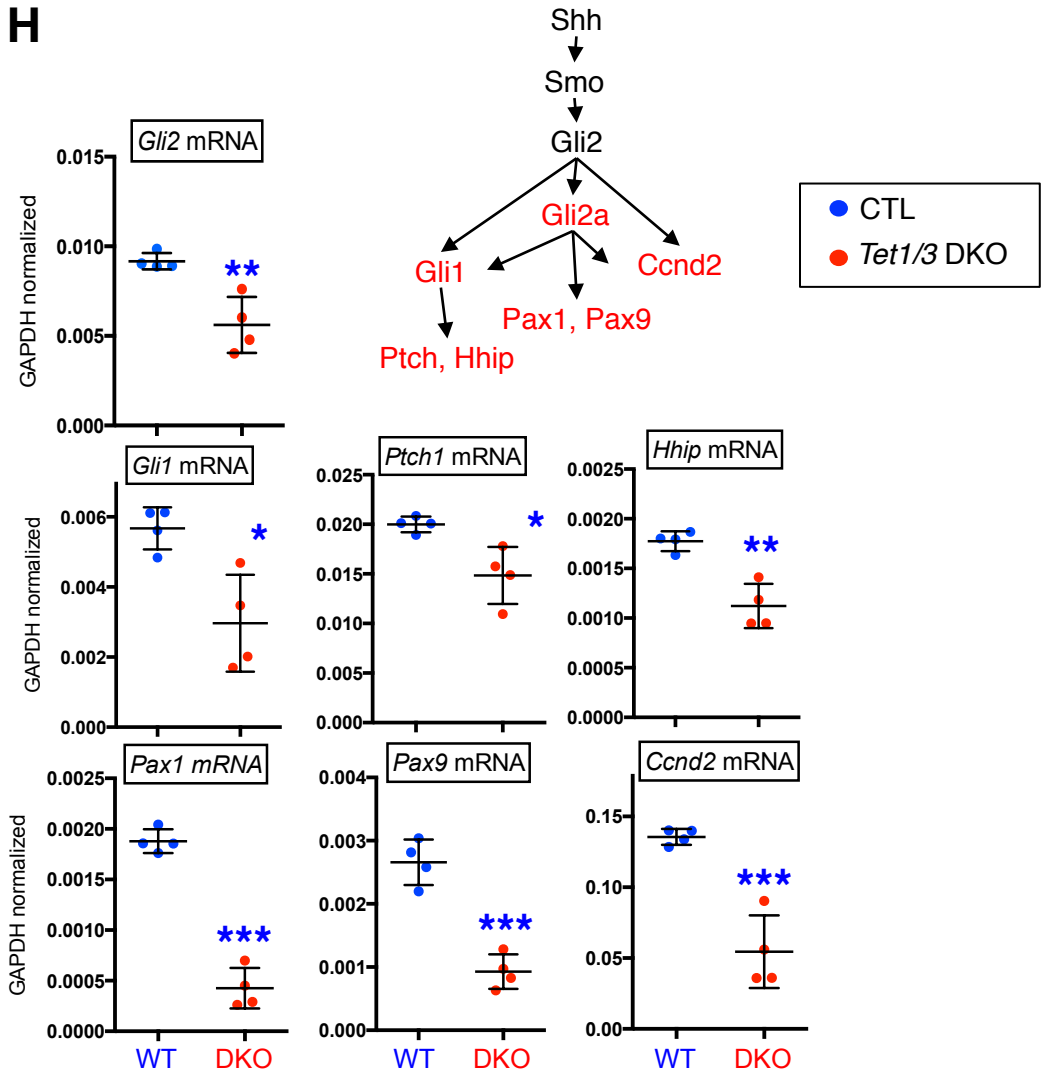

Figure S8. Genes whose expression is reproducibly downregulated in *Tet1/3* DKO compared to control embryos. (**A**) Gene ontology analysis using the 40 differentially expressed genes (adjusted p-value <0.01) identified the four indicated biological functions as the most significantly enriched categories. (**B**) Relative expression data for the 14 genes whose products are involved in regulating cellular lipid metabolism and cholesterol pathway. (**C**) The expression levels of *Srebf1/2* and *Scap* in individual blastocysts, plotted from RNA-seq data. (**D**, **E**) Immunocytochemistry of CTL and *Tet1/3* DKO blastocysts using Srebp2 (C-terminus) and Cdx2 antibodies (**D**) and Srebp2 antibody (N-terminus) and DAPI (**E**). The expression levels of Srebp2 protein are substantially lower in *Tet1/3 DKO* blastocysts compared to controls. (**F**) Near complete demethylation (C/5fC/5caC) of the *Srebp2* TSS and promoter regions in both CTL and Tet1/3 DKO E3.5 blastocysts (*top panel*) and E2.5 8-cell embryos (*bottom panel*). (**G**) Abnormal development of the central nervous system in Tet1/3 DKO E10.5 embryos compared to control (CTL) embryos, shown by cryosectioning and DAPI staining. Note the facial abnormalities and absence of the forebrain (*left, arrow*). (**H**) *Top,* Schematic of the Sonic Hedgehog (Shh) signaling pathway (adapted from (14)); *Bottom*, Downregulation of genes encoding the targets of the Shh signaling pathway *Gli1*, *Gli2*, *Ptch1*, *Hhip*, *Pax1*, *Pax9*, and *Ccnd2*, in four *Tet1/3* DKO E10.5 embryos compared to CTL, based on evaluation of mRNA expression by qPCR (* p-value<0.05, ** p-value<0.01; *** p-value <0.005). Each dot represents an average of technical triplicates from a single embryo.

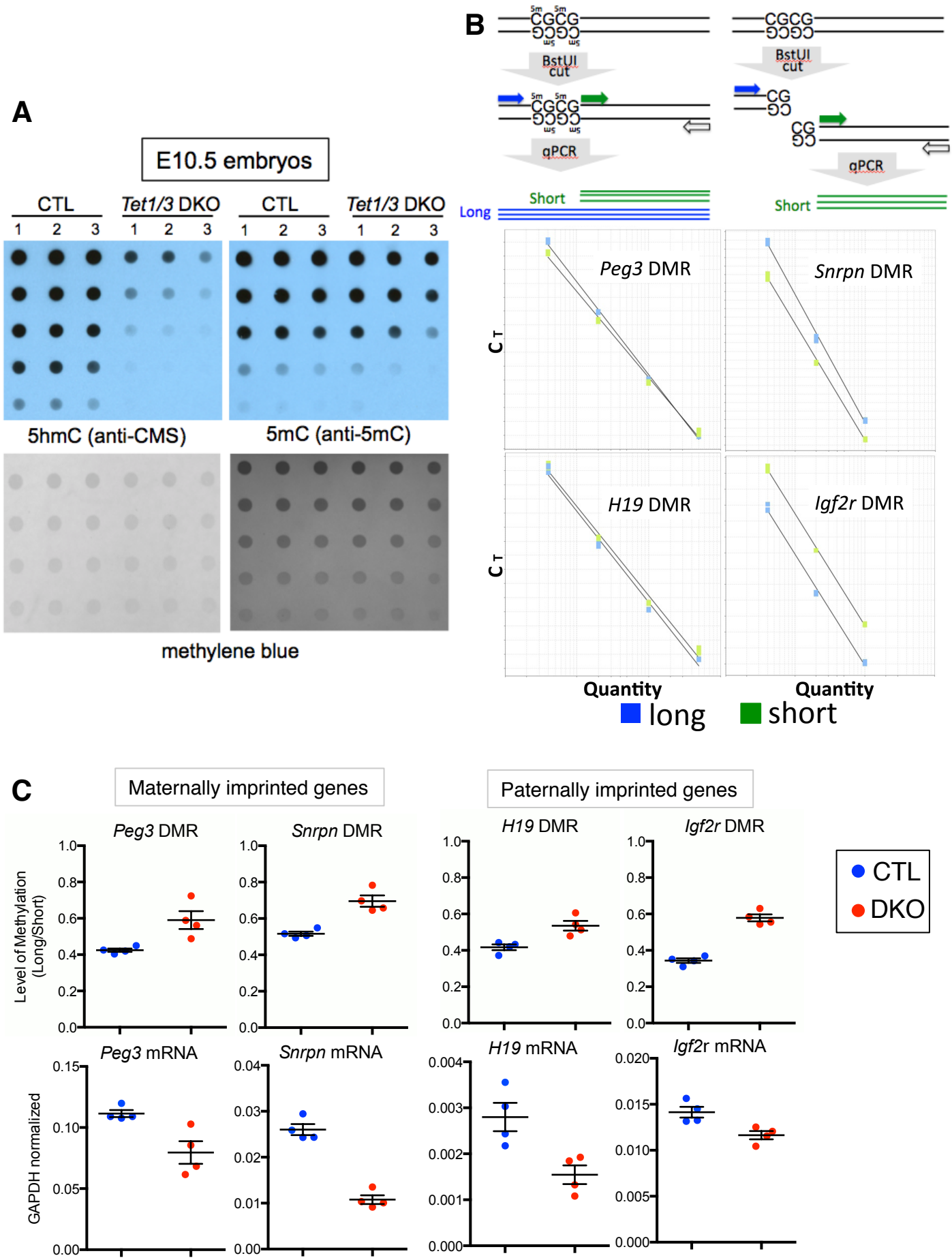
A
E10.5 embryos
CTL
Tet1/3 DKO
CTL
Tet1/3 DKO
1 2 3 1 2 3 1 2 3 1 2 3
5hmC (anti-CMS)
5mC (anti-5mC)
methylene blue
B
BstUI cut
qPCR
Long
Short
Short
Peg3 DMR
Snrpn DMR
H19 DMR
Igf2r DMR
CT
CT
Quantity
Quantity
long
short
C
Maternally imprinted genes
Paternally imprinted genes
Peg3 DMR
Snrpn DMR
H19 DMR
Igf2r DMR
Level of Methylation (Long/Short)
Peg3 mRNA
Snrpn mRNA
H19 mRNA
Igf2r mRNA
GAPDH normalized
CTL
DKO

Figure S9. *Tet1* and *Tet3* regulate imprinted genes in the late embryogenesis. (**A**) Severe reduction of 5hmC with little effect on 5mC levels in three *Tet1/3* DKO E10.5 embryos compared to CTL, based on DNA dot blots to quantify 5mC and CMS (cytosine 5-methylenesulfonate, the derivative formed by reaction of 5hmC with sodium bisulfite (11). Bottom panels show methylene blue staining of the same dot blots as a loading control. (**B**) *Top*, Schematic flow chart of methylation analysis using BstU1 (adapted from (13)); *bottom*, qPCR standard curves for 4 different DMR regions. (**C**) qPCR analyses of methylation levels (*top*) and mRNA levels (*bottom*) for paternally and maternally imprinted genes in 4 different CTL and *Tet1/3* DKO E10.5 embryos.

Table S1. *Tet1*KO embryos show partial embryonic lethality. The table shows the genotypes of pups produced by crossing *Tet1*$^{+/-}$ mice. A total of 30 litters were collected from 8 different crosses.

Tet1$^{+/-}$ X *Tet1*$^{+/-}$

Litter	*Tet1*$^{+/+}$	*Tet1*$^{+/-}$	*Tet1*$^{-/-}$	TOTAL
1		5		5
2		6		6
3		4		4
4		5		5
5	1	1	2	4
6		2	1	3
7	3	2		5
8	1	3		4
9	1	4		5
10		3	2	5
11	2	1	2	5
12	1	2	1	4
13	1	3	1	5
14	4	2		6
15		5		5
16	3	2	1	6
17	2	5		7
18	2	3		5
19	1	1	1	3
20	1	3		4
21	3	2		5
22	1	3		4
23	2	1		3
24	2	3		5
25		4		4
26		2		2
27		3		3
28	1	3	1	5
29	4	1		5
30	3	1		4
Total	**39**	**85**	**12**	**4.5 (Ave Litter)**
Ratio	*1 : 2.18 : 0.31*			

Table S2. Embryonic lethality *of Tet1/3* DKO embryos. Genotypes of pups produced by crossing *Tet1*$^{+/-}$*; Tet3*$^{+/-}$ mice. A total of 15 litters were evaluated.

Tet1$^{+/-}$*;Tet3*$^{+/-}$ X *Tet1*$^{+/-}$*;Tet3*$^{+/-}$

Litter	Size	Genotype
1	4	WT(1), *Tet1*$^{+/-}$(1), *Tet1*^{KO}(2)
2	2	*Tet1*$^{+/-}$*;Tet3*$^{+/-}$(2)
3	3	*Tet1*$^{+/-}$(1), *Tet1*$^{+/-}$*;Tet3*$^{+/-}$(2)
4	2	*Tet1*$^{+/-}$(1), *Tet1*^{KO}*;Tet3*$^{+/-}$(1)
5	5	WT(1), *Tet1*$^{+/-}$(1), *Tet1*$^{+/-}$*;Tet3*$^{+/-}$(3)
6	4	WT(2), *Tet1*$^{+/-}$(1), *Tet1*$^{+/-}$*;Tet3*$^{+/-}$(1)
7	4	WT(1), *Tet1*$^{+/-}$(1), *Tet3*$^{+/-}$(2)
8	3	WT(1), *Tet1*$^{+/-}$*;Tet3*$^{+/-}$(1),*Tet1*^{KO}(1)
9	5	WT(1), *Tet1*$^{+/-}$*;Tet3*$^{+/-}$(1),*Tet1*$^{+/-}$(1), *Tet3*$^{+/-}$(2)
10	2	*Tet1*$^{+/-}$*;Tet3*$^{+/-}$(2)
11	5	WT(1), *Tet1*$^{+/-}$(2), *Tet1*^{KO}(1), *Tet3*$^{+/-}$(1)
12	2	*Tet1*$^{+/-}$(1), *Tet3*$^{+/-}$(1)
13	2	*Tet1*$^{+/-}$(1), *Tet3*$^{+/-}$(1)
14	4	*Tet1*^{KO}(1), *Tet3*$^{+/-}$(1), *Tet1*$^{+/-}$*;Tet3*$^{+/-}$(2)
15	5	*Tet1*$^{+/-}$(3), *Tet1*^{KO}(1), *Tet3*$^{+/-}$(1)
Ave. Size	3.5	*Tet1* WT: Het: KO = 17: 28: 7 (1: 1.6: 0.4) *Tet3* WT: Het: KO = 28: 24: 0 (1: 0.9: 0)

Table S3. Quality control data for single-cell RNA-seq.

Library/Sample	Total Raw Reads	Reads Not Passing Filters	Reads Not Passing Filters %	Reads Passing Filters	Reads Passing Filters %	Total mapping to Spike-in Control	Total mapping to Spike-in Control %	Total mapping to tRNA/ rRNA	Total mapping to tRNA/rRNA %	Total mapping to Adaptors	Total mapping to Adaptors %	Total mapping to low-complexity reads	Total mapping to low-complexity reads %	Total mapping to reference	Total mapping to reference %	Total uniquely mapping Reads	Total uniquely mapping Reads %	Total unmapped	Total unmapped %
Library1:C4	6,916,857	681,025	9.85%	6,235,832	90.15%	430	0.01%	95,015	1.52%	0	0.00%	143,066	2.29%	5,477,746	87.84%	5,103,025	81.83%	519,575	8.33%
Library10:C6	8,181,847	969,457	11.85%	7,212,390	88.15%	1,637	0.02%	90,721	1.26%	0	0.00%	144,086	2.00%	6,276,619	87.03%	5,822,751	80.73%	699,327	9.70%
Library11:C14	8,292,540	1,032,379	12.45%	7,260,161	87.55%	2,983	0.04%	186,731	2.57%	0	0.00%	161,029	2.22%	6,243,174	85.99%	5,818,626	80.15%	666,244	9.18%
Library12:D2	6,016,934	587,547	9.77%	5,429,387	90.24%	821	0.02%	65,618	1.21%	0	0.00%	104,291	1.92%	4,754,929	87.58%	4,391,074	80.88%	503,728	9.28%
Library13:D9	9,242,595	1,118,947	12.11%	8,123,648	87.89%	1,938	0.02%	194,772	2.40%	0	0.00%	154,989	1.91%	7,023,394	86.46%	6,464,795	79.58%	748,555	9.22%
Library14:D14	9,300,113	1,071,406	11.52%	8,228,707	88.48%	2,017	0.03%	186,349	2.27%	0	0.00%	162,818	1.98%	7,070,560	85.93%	6,403,878	77.82%	806,963	9.81%
Library15:D20	7,585,703	896,849	11.82%	6,688,854	88.18%	155	0.00%	111,767	1.67%	0	0.00%	134,003	2.00%	5,928,763	88.64%	5,421,082	81.05%	514,166	7.69%
Library16:D27	11,027,614	1,366,280	12.39%	9,661,334	87.61%	1,689	0.02%	196,862	2.04%	0	0.00%	184,029	1.91%	8,210,676	84.99%	7,540,370	78.05%	1,068,078	11.06%
Library17:D32	7,636,116	931,081	12.19%	6,705,035	87.81%	1,947	0.03%	130,158	1.94%	0	0.00%	121,738	1.82%	5,829,277	86.94%	5,376,015	80.18%	621,915	9.28%
Library18:D37	9,212,512	1,022,738	11.10%	8,189,774	88.90%	828	0.01%	201,702	2.46%	0	0.00%	149,283	1.82%	7,064,050	86.26%	6,479,427	79.12%	773,911	9.45%
Library19:C7	8,287,875	963,850	11.63%	7,324,025	88.37%	1,618	0.02%	60,073	0.82%	0	0.00%	143,849	1.96%	6,460,535	88.21%	5,851,364	79.89%	657,950	8.98%
Library2:C11	6,303,010	651,980	10.34%	5,651,030	89.66%	1,318	0.02%	109,203	1.93%	0	0.00%	109,415	1.94%	4,925,166	87.16%	4,537,595	80.30%	505,928	8.95%
Library20:C15	6,853,283	860,695	12.56%	5,992,588	87.44%	2,184	0.04%	172,649	2.88%	0	0.00%	125,823	2.10%	5,120,759	85.45%	4,787,895	79.90%	571,173	9.53%
Library21:D4	7,339,287	793,674	10.81%	6,545,613	89.19%	1,501	0.02%	117,254	1.79%	0	0.00%	124,222	1.90%	5,722,409	87.42%	5,276,970	80.62%	580,227	8.86%
Library22:D10	9,019,307	1,078,676	11.96%	7,940,631	88.04%	3,088	0.04%	203,448	2.56%	0	0.00%	156,179	1.97%	6,848,135	86.24%	6,341,967	79.87%	729,781	9.19%
Library23:D15	7,540,189	890,088	11.81%	6,650,101	88.20%	870	0.01%	165,313	2.49%	0	0.00%	142,320	2.14%	5,726,537	86.11%	5,340,566	80.31%	615,061	9.25%
Library24:D21	7,634,388	893,649	11.71%	6,740,739	88.29%	1,284	0.02%	124,108	1.84%	0	0.00%	128,558	1.91%	5,859,870	86.93%	5,435,072	80.63%	626,919	9.30%
Library25:D28	9,799,325	1,203,147	12.28%	8,596,178	87.72%	2,304	0.03%	169,273	1.97%	0	0.00%	168,968	1.97%	7,355,268	85.56%	6,721,199	78.19%	900,365	10.47%
Library26:D33	9,241,188	1,079,344	11.68%	8,161,844	88.32%	3,205	0.04%	241,730	2.96%	0	0.00%	142,867	1.75%	7,001,195	85.78%	6,310,656	77.32%	772,847	9.47%
Library27:D38	6,576,598	738,030	11.22%	5,838,568	88.78%	754	0.01%	120,640	2.07%	0	0.00%	104,960	1.80%	5,200,419	89.07%	4,806,648	82.33%	411,795	7.05%
Library28:C9	7,446,992	654,664	8.79%	6,792,328	91.21%	895	0.01%	82,732	1.22%	0	0.00%	126,663	1.87%	5,991,962	88.22%	5,588,468	82.28%	590,076	8.69%
Library29:C16	8,155,254	720,184	8.83%	7,435,070	91.17%	1,733	0.02%	240,336	3.23%	0	0.00%	152,938	2.06%	6,250,418	84.07%	5,840,719	78.56%	789,645	10.62%
Library3:D1	9,019,307	1,078,676	11.96%	7,940,631	88.04%	3,088	0.04%	203,448	2.56%	0	0.00%	156,179	1.97%	6,848,135	86.24%	6,341,967	79.87%	729,781	9.19%
Library30:D6	6,723,875	522,151	7.77%	6,201,724	92.23%	1,036	0.02%	133,772	2.16%	0	0.00%	116,186	1.87%	5,474,543	88.28%	5,117,807	82.52%	476,187	7.68%
Library31:D11	9,937,703	874,561	8.80%	9,063,142	91.20%	2,761	0.03%	219,465	2.42%	0	0.00%	172,635	1.91%	7,832,267	86.42%	7,201,698	79.46%	836,014	9.22%
Library32:D16	7,019,965	585,465	8.34%	6,434,500	91.66%	1,742	0.03%	143,769	2.23%	0	0.00%	126,981	1.97%	5,575,392	86.65%	5,201,324	80.84%	586,616	9.12%
Library33:D24	6,396,929	537,848	8.41%	5,859,081	91.59%	1,583	0.03%	111,047	1.90%	0	0.00%	126,545	2.16%	5,112,563	87.26%	4,780,498	81.59%	507,343	8.66%
Library34:D29	9,976,390	876,319	8.78%	9,100,071	91.22%	2,437	0.03%	168,142	1.85%	0	0.00%	165,275	1.82%	7,801,823	85.73%	7,069,705	77.69%	962,394	10.58%
Library35:D34	8,281,854	740,056	8.94%	7,541,798	91.06%	866	0.01%	122,491	1.62%	0	0.00%	138,735	1.84%	6,643,774	88.09%	6,244,307	82.80%	635,932	8.43%
Library36:D39	6,576,515	540,563	8.22%	6,035,952	91.78%	480	0.01%	106,357	1.76%	0	0.00%	101,947	1.69%	5,108,519	84.64%	4,754,205	78.77%	718,649	11.91%
Library37:C10	7,167,350	700,400	9.77%	6,466,950	90.23%	1,206	0.02%	93,206	1.44%	0	0.00%	129,417	2.00%	5,627,325	87.02%	5,261,173	81.36%	615,796	9.52%
Library38:C17	6,790,880	693,005	10.21%	6,097,875	89.80%	774	0.01%	105,312	1.73%	0	0.00%	135,804	2.23%	5,259,845	86.26%	4,879,794	80.03%	596,140	9.78%
Library39:D7	5,907,088	528,606	8.95%	5,378,482	91.05%	938	0.02%	128,257	2.39%	0	0.00%	105,073	1.95%	4,708,461	87.54%	4,414,370	82.08%	435,753	8.10%
Library4:D8	9,349,419	918,497	9.82%	8,430,922	90.18%	1,419	0.02%	181,466	2.15%	0	0.00%	181,427	2.15%	7,102,774	84.25%	6,545,759	77.64%	963,836	11.43%
Library40:D12	7,427,033	709,619	9.56%	6,717,414	90.45%	1,116	0.02%	182,694	2.72%	0	0.00%	148,010	2.20%	5,544,385	82.54%	4,867,949	72.47%	841,209	12.52%
Library41:D17	7,025,000	664,134	9.45%	6,360,866	90.55%	2,186	0.03%	151,161	2.38%	0	0.00%	127,522	2.01%	5,543,654	87.15%	5,123,412	80.55%	536,343	8.43%
Library42:D25	6,016,934	587,547	9.77%	5,429,387	90.24%	821	0.02%	65,618	1.21%	0	0.00%	104,291	1.92%	4,754,929	87.58%	4,391,074	80.88%	503,728	9.28%
Library43:D30	7,686,440	784,278	10.20%	6,902,162	89.80%	2,655	0.04%	148,347	2.15%	0	0.00%	129,208	1.87%	6,040,547	87.52%	5,690,222	82.44%	581,405	8.42%
Library44:D35	6,752,129	665,060	9.85%	6,087,069	90.15%	382	0.01%	144,503	2.37%	0	0.00%	117,155	1.93%	5,109,156	83.94%	4,733,145	77.76%	715,873	11.76%
Library45:D40	6,941,139	637,383	9.18%	6,303,756	90.82%	1,282	0.02%	130,784	2.08%	0	0.00%	126,114	2.00%	5,431,459	86.16%	5,050,831	80.12%	614,117	9.74%
Library5:D13	5,909,580	572,477	9.69%	5,337,103	90.31%	764	0.01%	140,107	2.63%	0	0.00%	108,743	2.04%	4,603,237	86.25%	4,289,690	80.38%	484,252	9.07%
Library6:D18	6,917,816	661,316	9.56%	6,256,500	90.44%	1,154	0.02%	143,237	2.29%	0	0.00%	119,385	1.91%	5,463,810	87.33%	5,044,032	80.62%	528,914	8.45%
Library7:D26	9,817,020	974,649	9.93%	8,842,371	90.07%	617	0.01%	166,541	1.88%	0	0.00%	158,889	1.80%	7,722,357	87.33%	6,875,176	77.75%	793,967	8.98%
Library8:D31	7,556,654	738,610	9.77%	6,818,044	90.23%	3,980	0.06%	123,548	1.81%	0	0.00%	133,249	1.95%	5,954,730	87.34%	5,534,141	81.17%	602,537	8.84%
Library9:D36	6,380,434	571,987	8.97%	5,808,447	91.04%	989	0.02%	140,416	2.42%	0	0.00%	110,561	1.90%	4,987,300	85.86%	4,626,438	79.65%	569,181	9.80%

Table S4. Quality control data for single-embryo RNA-seq.

Sample	Yield (IVbases)	%PF	Uniquely mapped #Reads	% of raw clusters per lane	% of >= Q30 Bases (PF)	Mean Quality Score (PF)
CTL1	3461	87.72	16015620	7.76	84.6	33.47
CTL2	3253	91.87	19392099	6.96	84.61	33.45
CTL3	2442	84.44	20545177	5.69	84.64	33.54
DKO1	3680	92.04	14947743	7.86	84.65	33.49
DKO2	4162	91.37	14087557	8.96	83.29	33.06
DKO3	3675	91.49	10897802	7.9	83.3	33.07
DKO4	4477	91.46	16224767	9.63	83.42	33.1
DKO5	4819	92.55	17949154	10.24	84.75	33.48

Table S5. Quality control data for single embryo RRBS.

	Total reads	Mapped reads	% mapping	1x covered CpGs	10x covered GpGs	Conversion Rate
CTL a	19335199	8732537	45.16	1822218	833660	0.986
CTL b	17690459	7366240	41.63	1887471	924783	0.990
CTL c	15888366	6966017	43.84	2169143	750820	0.992
DKO a	16842069	8642821	51.31	1782422	930057	0.991
DKO b	13985522	4846425	34.65	1284160	289727	0.982
DKO c	23850991	11092011	46.50	1585596	780420	0.989
DKO d	17577103	7960881	45.29	725127	247318	0.982
DKO e	16332894	8839751	54.12	1497757	659754	0.987

Dataset S1. Single-embryo RNA-seq data analyses of control and Tet1/3 DKO embryos and list of genes identified in **Fig. 4B and 4G**.

Supporting Information References

1. Lewandoski M, Wassarman KM, & Martin GR (1997) Zp3-cre, a transgenic mouse line for the activation or inactivation of loxP-flanked target genes specifically in the female germ line. *Current biology : CB* 7(2):148-151.

2. Sadate-Ngatchou PI, Payne CJ, Dearth AT, & Braun RE (2008) Cre recombinase activity specific to postnatal, premeiotic male germ cells in transgenic mice. *Genesis* 46(12):738-742.

3. Yamaguchi S, Shen L, Liu Y, Sendler D, & Zhang Y (2013) Role of Tet1 in erasure of genomic imprinting. *Nature* 504(7480):460-4.

4. Hackett JA*, et al.* (2013) Germline DNA demethylation dynamics and imprint erasure through 5-hydroxymethylcytosine. *Science* 339(6118):448-452.

5. Gu TP*, et al.* (2011) The role of Tet3 DNA dioxygenase in epigenetic reprogramming by oocytes. *Nature* 477(7366):606-610.

6. Anders S & Huber W (2010) Differential expression analysis for sequence count data. *Genome Biol* 11(10):R106.

7. Biase F, Cao X, & Zhong S (2014) Cell fate inclination within 2-cell and 4-cell mouse embryos revealed by single-cell RNA sequencing. *Genome Res* 24(11):1787-96.

8. Yoav Benjamini & Hochberg Y (1995) Controlling the False Discovery Rate: A Practical and Powerful Approach to Multiple Testing. *Journal of the Royal Statistical Society. Series B (Methodological)* 57(1):289-300.

9. Langmead B, Trapnell C, Pop M, & Salzberg SL (2009) Ultrafast and memory-efficient alignment of short DNA sequences to the human genome. *Genome Biol* 10(3):R25.

10. Krueger F & Andrews SR (2011) Bismark: a flexible aligner and methylation caller for Bisulfite-Seq applications. *Bioinformatics* 27(11):1571-1572.

11. Ko M*, et al.* (2011) Impaired hydroxylation of 5-methylcytosine in myeloid cancers with mutant TET2. *Nature* 468(7325):839-843.

12. Huang Y, Pastor WA, Zepeda-Martinez JA, & Rao A (2012) The anti-CMS technique for genome-wide mapping of 5-hydroxymethylcytosine. *Nat Protoc* 7(10):1897-1908.

13. Lorthongpanich C*, et al.* (2013) Single-cell DNA-methylation analysis reveals epigenetic chimerism in preimplantation embryos. *Science* 341(6150):1110-1112.

14. Buttitta L, Mo R, Hui CC, & Fan CM (2003) Interplays of Gli2 and Gli3 and their requirement in mediating Shh-dependent sclerotome induction. *Development* 130(25):6233-6243.